Ecological Modelling 500 (2025) 110954

Contents lists available at ScienceDirect

Ecological Modelling

journal homepage: www.elsevier.com/locate/ecolmodel

A multi-objective optimization model for cropland design considering profit, biodiversity, and ecosystem services

Caleb H. Geissler [a,b,*], Nathan L. Haan [c,d], Bruno Basso [d,e], Ames Fowler [d,e], Douglas A. Landis [d,f], Tyler J. Lark [g,h], Christos T. Maravelias [a,b,i]

[a] *Department of Chemical and Biological Engineering, Princeton University, Princeton, NJ, 08544, United States*
[b] *DOE Great Lakes Bioenergy Research Center, United States*
[c] *Department of Entomology, University of Kentucky, Lexington, KY 40508, United States*
[d] *DOE Great Lakes Bioenergy Research Center, Michigan State University, United States*
[e] *Department of Earth and Environmental Science, Michigan State University, East Lansing, MI, 48823, United States*
[f] *Department of Entomology, Michigan State University, East Lansing, MI 48823, United States*
[g] *Center for Sustainability and the Global Environment, Nelson Institute for Environmental Studies, University of Wisconsin-Madison, Madison, WI, 53726, United States*
[h] *DOE Great Lakes Bioenergy Research Center, University of Wisconsin-Madison, United States*
[i] *Andlinger Center for Energy and the Environment, Princeton University, Princeton, NJ, 08544, United States*

ARTICLE INFO

Keywords:
Biodiversity
Ecosystem services
Mathematical optimization
Multi-objective optimization
MIQCP

ABSTRACT

More sustainable agricultural methods are needed to alleviate the decreases in biodiversity and ecosystem services that have occurred because of industrial agriculture. One such method is the inclusion of alternative crops into croplands that can support biodiversity, reduce erosion and chemical runoff, and sequester carbon in the soil. However, the question of where such crops should be planted to balance competing economic and environmental objectives remains open. To this end, we develop a mixed-integer quadratically constrained program to optimize the layout of a cropland considering economic, biodiversity, greenhouse gas emissions, and water quality objectives. We include spatially varying fertilization as a decision variable in addition to crop establishment location. We further include the effect of core area and edges between different crops on biodiversity. To demonstrate the applicability of the model, we apply it to an example field, showing how the optimal cropland design changes as a decision-maker prioritizes different objectives and as edges have different impacts on biodiversity.

1. Introduction

Increases in industrial agriculture have provided high crop yields necessary to feed a growing population but have led to significant degradation to the environment (Butchart et al., 2010). These negative effects include losses of native wildlife and ecosystem services (Sala et al., 2000). Key ecosystem services particularly impacted by agricultural expansions include greenhouse gas (GHG) balance (Houghton et al., 2012), water quality regulation (Jiao et al., 2011), erosion control (Karlen et al., 2013), and pollination (Kremen et al., 2002). While corn is a dominant annual crop in the US Midwest and the business-as-usual bioenergy crop with ~40 % of harvest allocated to producing ethanol (*U.S. Bioenergy Statistics*, 2024), there are alternative crops that can be grown for other markets, such as perennial bioenergy feedstocks, which are more environmentally friendly. For example, switchgrass (*Panicum virgatum*) is a perennial North American native grass with several varieties that have been bred specifically for bioenergy applications. Reconstructed prairies emulate biodiverse native grasslands characteristic of the US Midwest prior to Euro-American colonization and have been proposed as an alternative to annual and/or monoculture sources of bioenergy (Tilman et al., 2006). Empirical studies have found that the introduction of strips of perennial vegetation into cropland can significantly improve the biodiversity and delivery of key ecosystem services of the cropland (Kemmerling et al., 2022; Schulte et al., 2017). One approach for more carefully selecting pieces of land to set aside for these purposes is using remote sensing images, which allow for the identification of consistently underproducing areas. If these areas were planted with unfertilized native vegetation, including bioenergy feedstocks, they

---

* Corresponding author.
E-mail address: geissler@princeton.edu (C.H. Geissler).

https://doi.org/10.1016/j.ecolmodel.2024.110954
Received 12 July 2024; Received in revised form 8 November 2024; Accepted 16 November 2024

could provide greater ecosystem services and economic benefits to farmers while reducing nutrient losses and creating habitat for native species (Basso, 2021; Basso & Antle, 2020). Taking the insights from these studies and using modeling of the effect of cropland composition and configuration on biodiversity and ecosystem services can allow for improved cropland design that balances crop production and environmental sustainability.

Because biodiversity has been declining for many years, it has received significant attention (Butchart et al., 2010; Camm et al., 2007). An approach to combat this decline is by setting aside certain areas to be protected from development and instead be preserved to provide a habitat for species of interest. Determining what areas should be protected can be nontrivial, and conversation planning tools have been developed over decades to help generate conservation plans. One approach to aid systematic conservation planning in support of biodiversity goals is to select planning units within a landscape to protect or revert to natural cover (Ball & Possingham, 2000; Basso, 2021; Billionnet, 2013). Potential objectives for such conservation planning problems include maximizing the biodiversity benefits from a given area of protection, minimizing the cost of establishing a reserve of a given area, and maximizing the compactness of a reserve (Margules et al., 1988; Weerasena et al., 2023). To correlate area with biodiversity, or the survival of a specific species, biological models of species persistence have been developed (Olsson et al., 2021; Polasky et al., 2005; Strassburg et al., 2019). These models can include factors for the size of individual protected areas, the distances between them, the varying quality of habitat provided by different crops, and the dispersal of the given species to predict the likelihood that a species will persist in the landscape. Such a model, developed by (Polasky et al., 2005), includes a penalty for habitat fragmentation, though notably does not include any potential benefit that habitat fragmentation could have on specific species.

Another key factor in the sustainability of agriculture is the maintenance of ecosystem services. Ecosystem services such as GHG sequestration and water quality are determined by complex interactions between soil, climate, genetics, and land management. Detailed process-based models have been developed to simulate these interactions and thereby predict carbon, water, and nutrient fluxes in the environment (Basso & Ritchie, 2015; Stanford University et al., 2023). These models can provide valuable insights, but their performance is dependent on the quality and representativeness of the inputs fed into the models. Furthermore, they can be computationally demanding to run. When parametrized with high-quality data, they can provide detailed results when a land cover type is specified, such as in the case of scenario studies (Adams et al., 2016; Basso et al., 2018; Law et al., 2015; Nelson et al., 2009), but are difficult to incorporate into already complex optimization models.

Some researchers have examined the design of landscapes considering economic, biodiversity, or ecosystem services objectives. Brosi et al. (2008) developed a model to design a landscape integrating economic and pollination objectives. Williams et al. (2020) applied a simple allocation model with static agriculture production, biodiversity, and ecosystem service values for each planning unit to the Orinoquia in Colombia. Polasky et al. (2008) used a detailed biodiversity model to design a landscape that balances profit and biodiversity in the Willamette Basin in Oregon, USA. Kennedy et al. (2016) built on this model and studied profit from cattle ranching or sugarcane production, biodiversity, and water quality in the Ribierão São Jerônimo watershed in Brazil. While these studies provide insightful results for large regions, they use highly nonlinear models that are solved using local search techniques, which cannot guarantee (near)-optimal solutions. Furthermore, even the models that have fine resolution do not include edge effects, which have been shown to impact biodiversity (Reino et al., 2009; Schlegel, 2022; Vallejos et al., 2024).

To address the gaps in the literature mentioned above, we present a multi-objective mixed-integer quadratically constrained programming (MIQCP) model, which can be solved to optimality, for an area of cropland considering profit, biodiversity, GHG emissions, and water quality. We include the impact of habitat configuration, represented through the amount of edges between different crops, on the objectives, and include fertilization as a decision variable. While the primary contribution of this paper is the model itself, we show how the model can be used to determine optimal crop establishment and fertilization decisions for a variety of different weights in the objective function and with different considerations of edge impacts.

2. Mathematical formulation

We use lowercase Greek letters for parameters, uppercase italic Latin letters for variables, lowercase italic Latin letters for indices, and uppercase bold Latin letters for sets. We introduce the full set notation the first time that a set is introduced. To keep the equations more compact, set membership is not explicitly provided in the equation domain when the equation is written for the entire set. For example, Eq. (1) is written for $j \in \mathbf{J}$. We begin in Section 2.1 without considering the impact that an edge between two adjacent crops has on each objective. Equations considering edge impacts are formulated in Section 2.2.

2.1. No edge impacts

The model has five groups of constraints, outlined in the following subsections.

2.1.1. Patch size

We consider a cropland separated into cells $i \in \mathbf{I}$ and a set of potential crops to plant $j \in \mathbf{J}$. It may be known *a priori* that certain crops must be planted in certain cells, denoted by a pre-specified crop establishment parameter $\chi_{i,j}$,

$$X_{i,j} = \chi_{i,j}, \;\; i \in \mathbf{I}_j^{FX}, \; j \tag{1}$$

where $X_{i,j}$ is a binary variable indicating the planting of a given crop in each cell and $\mathbf{I}_j^{FX}$ is the subset of cells for which it is pre-specified that crop j will be planted.

For all cells, an essential decision is what crop to plant,

$$\sum_j X_{i,j} = 1, \;\; i \tag{2}$$

To calculate biodiversity, it is necessary to know the size of a series of connected cells (rooks-case) with the same crop planted, which we refer to as a patch. Based on prior work in the literature, we use flow-based contiguity constraints to calculate the size of each patch, as outlined in the following equations (Shirabe, 2009). In this formulation, each cell supplies one unit of flow, which goes to a cell that is a sink for that patch. Thus, the total flow into the sink represents the total number of cells in the patch. Flow $F_{i,i',j}$ can occur between adjacent cells $(i, i') \in \mathbf{I}_i^A$ with the same crop planted. Flow cannot occur between cells with different crops, which is enforced and bounded by the following equation,

$$\delta_j = |\mathbf{I}| - \sum_{i' \in \mathbf{I}_{j'}^{FX}, j', j' \neq j} \chi_{i',j'}, \; j \tag{3}$$

$$\sum_{i' \in \mathbf{I}_i^A} F_{i,i',j} \leq (\delta_j - 1) X_{i,j}, \;\; i, \; j \tag{4}$$

where δ_j is an upper bound for flows of crop j. If no cells are fixed *a priori*, then the upper bound on flows is merely the total number of cells. However, the upper bound of flows for a crop is reduced by the total number of cells pre-specified to have a different crop planted.

We specify one of the cells in a patch to be a sink into which the flows within the patch accumulate. A cell can only be a sink for a patch of a given crop if that crop is planted in that cell,

$$Z_{i,j} \le X_{i,j},\ i,\ j \tag{5}$$

where $Z_{i,j}$ is a binary variable indicating that a cell is the sink of a patch for crop j.

Each cell produces one unit of flow, so the flow out of a cell minus the flow into that cell (the lefthand side of Eq. (6)) is 1 if that crop is planted there and that cell is not the sink. If the cell is the sink, then Eq. (6) enforces that the flow into the cell plus the one unit of flow supplied by the cell equals the total number of cells in the patch,

$$\sum_{i' \in \mathbf{I}_i^A} F_{i,i',j} - \sum_{i' \in \mathbf{I}_i^A} F_{i',i,j} = X_{i,j} - F_{i,j}^{SINK},\ i,\ j \tag{6}$$

where $F_{i,j}^{SINK}$ is the number of cells in that patch if cell i is the sink for the patch.

To ensure that $F_{i,j}^{SINK}$ is 0 when cell i is not the sink for the patch, Eqs. (7)–(9) are introduced. The total flow into the sink will be 1 less than the number of cells in the patch, so $Z_{i,j}$ is added to ensure that $F_{i,j}^{SINK}$ is calculated correctly,

$$\sum_{i' \in \mathbf{I}_i^A} F_{i',i,j} + Z_{i,j} = F_{i,j}^{SINK} + \widehat{F}_{i,j}^{SINK},\ i,\ j \tag{7}$$

where $\widehat{F}_{i,j}^{SINK}$ is a dummy variable for flows into cells that are not sinks.

Eqs. (8) and (9) enforce that $F_{i,j}^{SINK}$ is 0 when cell i is not the sink for the patch, in which case $\widehat{F}_{i,j}^{SINK}$ becomes positive,

$$F_{i,j}^{SINK} \le \delta_j Z_{i,j},\ i,\ j \tag{8}$$

$$\widehat{F}_{i,j}^{SINK} \le \delta_j \left(1 - Z_{i,j}\right),\ i,\ j \tag{9}$$

To improve solution time, we add a redundant constraint that the sum of all flows for a given crop into sinks must equal the total number of cells with that crop planted,

$$\sum_i F_{i,j}^{SINK} = \sum_i X_{i,j},\ j \tag{10}$$

Fig. 1 shows an example of the activation of the flow and crop establishment variables.

2.1.2. Biodiversity

We consider different species groups $k \in \mathbf{K}$ (e.g. birds, bees). We include a critical area requirement $\zeta_{j,k}$ specific to each combination of crop and species group. This indicates the minimum size of a patch that contributes to the viability of species within the species group. A species group with a strictly positive critical area requirement means that patches below that critical area requirement do not contribute to the biodiversity of that species group. If a species group has a critical area requirement smaller than the area of a single cell, even one cell of that crop increases the biodiversity of that species group. The dummy variable $\widehat{A}_{i,j,k}^{EFF}$ and binary variable $W_{i,j,k}$ (which indicates if a patch is large enough to increase the biodiversity of a species group) ensure that the effective area of a patch, $A_{i,j,k}^{EFF}$, is always nonnegative. The area of a patch is simply the number of cells in the patch multiplied by the area of a cell, α,

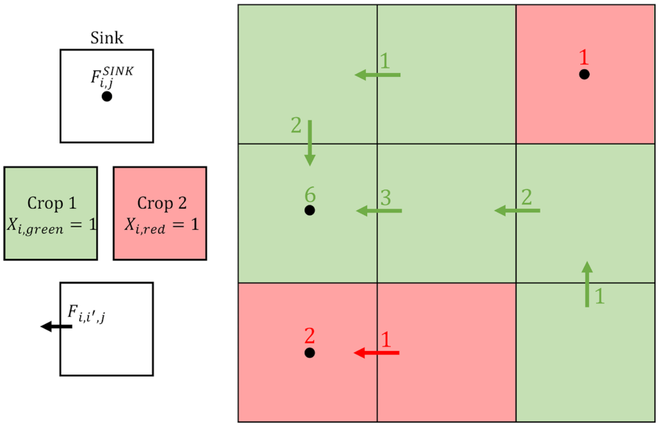

Fig. 1. Example of flow and binary variable values, where $\mathbf{I} = \{\text{green}, \text{red}\}$; for a cell with the green crop planted, all flow and binary variables for red crops have a value of 0, and vice versa.

$$\alpha F_{i,j}^{SINK} = A_{i,j,k}^{EFF} + \widehat{A}_{i,j,k}^{EFF},\ i, j, k \tag{11}$$

Variable $A_{i,j,k}^{EFF}$ is the area of the patch if the area is greater than $\zeta_{j,k}$ and if cell i is a sink for crop j (i.e. when $W_{i,j,k} = 1$), and 0 otherwise. This is enforced through the following,

$$\zeta_{j,k} W_{i,j,k} \le A_{i,j,k}^{EFF} \le \alpha \delta_j W_{i,j,k},\ i, j, k \tag{12}$$

If $W_{i,j,k} = 0$, dummy variable $\widehat{A}_{i,j,k}^{EFF}$ takes the value necessary to satisfy Eq. 11,

$$\widehat{A}_{i,j,k}^{EFF} \le \zeta_{j,k}\left(1 - W_{i,j,k}\right),\ i, j, k \tag{13}$$

To improve solution time, we also explicitly add constraints forcing $W_{i,j,k}$ and $A_{i,j,k}^{EFF}$ to be zero when $Z_{i,j}$ is zero,

$$W_{i,j,k} \le Z_{i,j},\ i,\ j, k \tag{14}$$

$$\sum_k A_{i,j,k}^{EFF} \le \delta_j Z_{i,j},\ i,\ j \tag{15}$$

Increasing habitat area has been well-documented to increase the probability of a species being present in a nonlinear manner (He et al., 2022). The relationship between the effective area and the fraction of species in a group expected to be present in crop j ($B_{j,k}$) is described by a species-area curve that saturates at high areas. Because $B_{j,k}$ will be maximized, we use linear segments, $l \in \mathbf{L}$, to replicate the species-area curve based on the total effective area for each species $A_{j,k}^{TOT}$ while maintaining linearity, and $A_{j,k}^{TOT}$ is disaggregated into $|\mathbf{L}|$ segments, denoted by $\widetilde{A}_{j,k,l}^{TOT}$,

$$A_{j,k}^{TOT} = \sum_i A_{i,j,k}^{EFF},\ j, k \tag{16}$$

$$A_{j,k}^{TOT} = \sum_l \widetilde{A}_{j,k,l}^{TOT},\ j, k \tag{17}$$

Variable $\widetilde{A}_{j,k,l}^{TOT}$ is constrained to be less than the upper bound for each segment l,

$$\widetilde{A}_{j,k,l}^{TOT} \le \mu_{j,k,l}^1,\ j, k,\ l \tag{18}$$

where $\mu_{j,k,l}^1$ is the upper bound on the domain of each linear segment of the species-area curve, and $\mu_{j,k,l}^2$ is the slope of each linear segment.

Variable $B_{j,k}$ can then be calculated by the sum of the products of the disaggregated total area within each segment and the slope associated with that segment,

$$B_{j,k} = \sum_l \mu_{j,k,l}^2 \widetilde{A}_{j,k,l}^{TOT},\ j, k,\ l \tag{19}$$

Because increasing the total area has diminishing returns, the area in $A_{j,k}^{TOT}$ will always be allocated to the disaggregated segments in order from left to right in Fig. 2.

The model determines what fraction of species within a species group are present somewhere in the cropland (B_k^{TOT}) but does not track if one

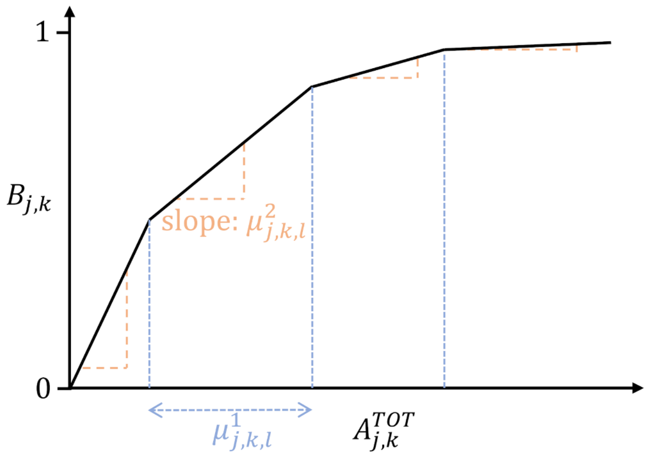

Fig. 2. Illustration of linear approximation of species-area curve.

specific species is guaranteed to be present. Instead, we assume that the presence of species in habitats associated with each crop is random. Thus, as seen in Olsson et al., (2021), we calculate B_k^{TOT} based on the expected fraction of species that would be present somewhere in the cropland,

$$B_k^{TOT} = 1 - \prod_j \left(1 - B_{j,k}\right),\ k \tag{20}$$

The above equation can be used directly in a MIQCP model if only two crops are considered. If more than two crops are considered, then a model using the above equation must be solved with a general MINLP solver, which may be slower. However, the model can be solved by a, more efficient, MIQCP solver if the equation is reformulated as a series of bilinear terms,

$$\widehat{B}_{j,k} = \left(1 - B_{j,k}\right),\ j \in \mathbf{J}^F, k \tag{21}$$

$$\widehat{B}_{j,k} = \left(1 - B_{j,k}\right)\widehat{B}_{j-1,k},\ j \in \mathbf{J} \backslash \mathbf{J}^F, k \tag{22}$$

$$B_k^{TOT} = 1 - \widehat{B}_{j,k},\ j \in \mathbf{J}^L, k \tag{23}$$

where $\widehat{B}_{j,k}$ is a dummy variable and $\mathbf{J}^F$ and $\mathbf{J}^L$ are singleton subsets of the first and last crops in **J**, respectively.

If only two crops are considered, a convex hull linear approximation can also be used, which is presented in Equations S6-S24 in the Supplementary Material. While this approximation introduces additional binary variables, it converts the model into a mixed-integer linear program, which can be solved potentially faster and with a greater variety of solvers.

2.1.3. *Profit*

Set **J** includes crops that are harvested and that are not harvested. Some crops may be either harvested or left year-round to support biodiversity and ecosystem services (e.g. perennial systems that harbor overwintering beneficial insects or grassland birds). For these crops, the biodiversity benefit depends on whether the crop is harvested, so one element in set **J** would correspond to the unharvested crop, and another would correspond to that same crop when it is harvested. For example, set **J** might consist of corn (C), unharvested switchgrass (USW), and harvested switchgrass (HSW), and parameters such as $\mu^1_{j,k,l}$ and $\mu^2_{j,k,l}$ would differ between USW and HSW. For the crops that are harvested ($j \in \mathbf{J}^C$), we also consider the amount of fertilizer applied to a crop in a given cell, $N_{i,j}$, and assume a linear increase in crop yield with fertilizer application, up to a maximum. As detailed in Section 2.1.5, water flowing between cells due to differences in elevation can carry runoff components $m \in \mathbf{M}$, such as pesticides and fertilizer. Nitrogen from the fertilizer (referred to as a singleton subset $m \in \mathbf{M}^N$) can be absorbed by a crop, increasing its yield. Therefore, the amount of a crop produced in a cell, $P_{i,j}$, can be calculated based on its expected baseline yield, $\psi_{i,j}$, and the amount of nitrogen taken up by a crop in a cell, $C^R_{i,j,m}$. The calculation of $C^R_{i,j,m}$ is shown in Section 2.1.5.

$$P_{i,j} = \psi_{i,j} X_{i,j} + \psi^F_{i,j} C^R_{i,j,m},\ i,\ j \in \mathbf{J}^C, m \in \mathbf{M}^N \tag{24}$$

$$N_{i,j} \le \beta^F_{i,j} X_{i,j},\ i,\ j \in \mathbf{J}^C \tag{25}$$

where $\psi_{i,j}$ is the baseline yield of a crop in a cell, $\psi^F_{i,j}$ is the additional yield per unit of fertilizer applied, $\beta^F_{i,j}$ is the upper bound on how much fertilizer can be applied to a crop in a cell, and $\mathbf{M}^N$ is a singleton subset of a nitrogen runoff.

The total profit of the cropland, R, is,

$$R = \sum_{i,j \in \mathbf{J}^C} \left[\pi^S_j P_{i,j} - \pi^N N_{i,j}\right] - \sum_{i,j} \pi^C_{i,j} X_{i,j} \tag{26}$$

where π^S_j is the price of a crop, π^N is the price of purchasing and applying fertilizer, and $\pi^C_{i,j}$ is the total cost of planting and harvesting (if applicable) a crop. We assume land and equipment ownership by the producer so that fixed costs are approximately zero.

2.1.4. *Greenhouse gas emissions*

For each cell, the GHG balance G_i is a function of crop establishment and fertilization decisions. Each crop has different energy consumption to plant and harvest as well as different interactions with the soil, which leads to different GHG balances. Fertilization has multiple effects on the GHG balance. First, the production and application of fertilizer requires energy input that leads to emissions, described by ϕ^F. Second, fertilization can lead to increased soil organic carbon sequestration, but also increased NO_x generation. The balance of these two effects for each combination of cell and crop is described by $\phi^E_{i,j}$.

$$G_i = \sum_j \left[\phi^C_{i,j} X_{i,j} + \left(\phi^E_{i,j} + \phi^F\right) N_{i,j}\right],\ i \tag{27}$$

where $\phi^C_{i,j}$ is the crop- and cell-specific emission factor.

2.1.5. *Water quality*

For water quality, the mass of dissolved components in water runoff can be produced and removed in each cell depending on what crop is planted and how much fertilizer is applied. For example, the application of fertilizer can lead to excess nitrogen in the water that could flow to adjacent cells, while crops like prairie can remove some of the excess nitrogen that flows into its cell. Many of the parameters introduced in this section vary with soil type and amount of rainfall, but we assume these to be constant at the field level. Runoff components flow between cells based on the difference in elevation and can either infiltrate into the soil or exit the cropland by flowing over the boundary of the cropland. A visual summary of the relevant variables is presented in Fig. 3. We note that these flows of components are distinct from the flow variables $F_{i,i',j}$ that calculate the size of patches.

The amount of runoff produced in each cell, $C^P_{i,m}$, is based on what crop is planted in that cell and how much fertilizer is applied,

$$C^P_{i,m} = \sum_{j \in \mathbf{J}^C} \left[\kappa^P_{j,m} X_{i,j} + \kappa^N_{j,m} N_{i,j}\right],\ i,\ m \in \mathbf{M}^N \tag{28}$$

$$C^P_{i,m} = \sum_j \kappa^P_{j,m} X_{i,j},\ i,\ m \in \mathbf{M} \backslash \mathbf{M}^N \tag{29}$$

where $\kappa^P_{j,m}$ is the amount of runoff components produced by the agricultural chemicals applied to a crop, which could be none, and $\kappa^N_{j,m}$ is the

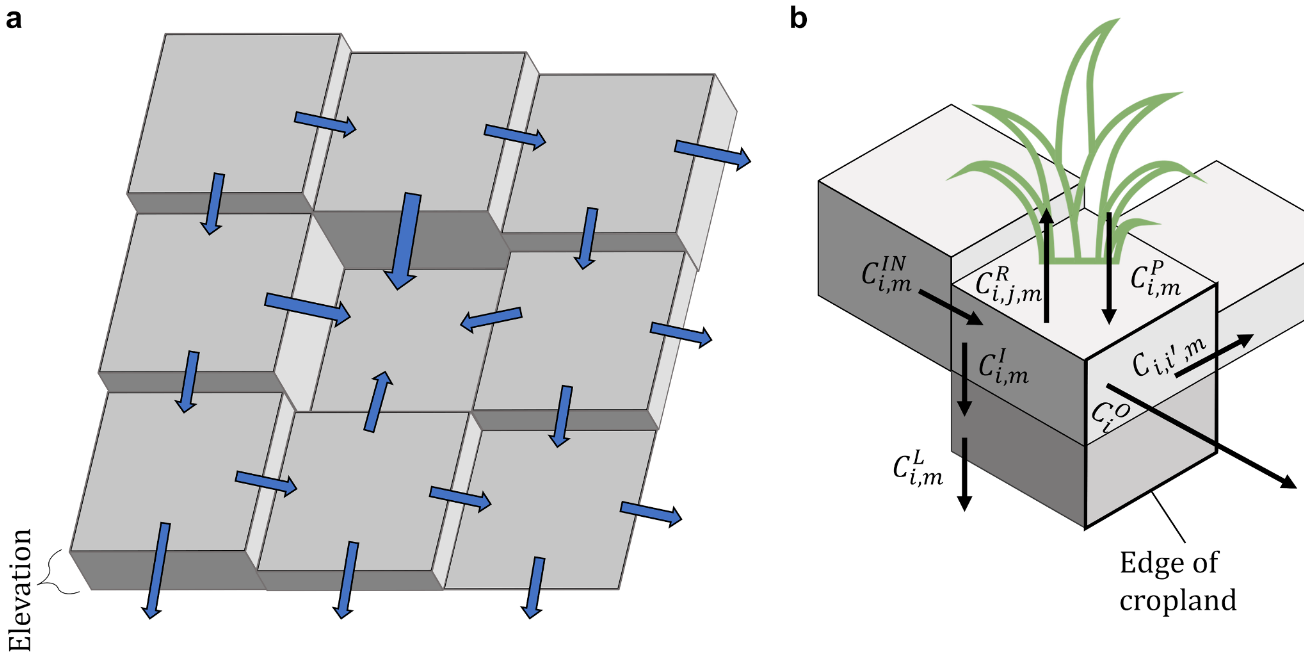

Fig. 3. Example cropland with potential directions for flows (a) and runoff component flow balance for one cell (b). In (b), $C_{i,m}^{P}$ is the runoff produced in a cell, $C_{i,j,m}^{R}$ is the runoff removed in a cell, $C_{i,m}^{IN}$ is runoff flowing into a cell, $C_{i,i',m}$ is runoff flowing between cells, $C_{i,m}^{I}$ is the runoff infiltrating the soil, $C_{i,m}^{L}$ is the runoff leaching into the soil, and C_{i}^{O} is the runoff exiting the cropland.

amount of runoff component produced per unit of fertilizer applied to a given crop.

Some crops may also remove runoff components in the cells in which they are planted. We assume these crops remove a fraction $\rho_{j,m}^{R}$ of the runoff components in a cell up to an upper bound $\theta_{j,m}^{R}$. To maintain linearity, binary variable $V_{i,m}$ is introduced, which indicates when runoff component removal is limited by the upper bound. The following four equations enforce that the amount of runoff components removed is the minimum between the given fraction of runoff component entering the cell and the absolute upper bound,

$$C_{i,j,m}^{R} \leq \rho_{j,m}^{R}\left(C_{i,m}^{IN} + C_{i,m}^{P}\right), \; i, \; j, \; m \tag{30}$$

$$C_{i,j,m}^{R} \leq \theta_{j,m}^{R} X_{i,j}, \; i, \; j, \; m \tag{31}$$

where $C_{i,m}^{IN}$ is the total flow of runoff components into a cell.

To ensure that $C_{i,j,m}^{R}$ is nonzero when needed, a big-M formulation is used with binary variable $V_{i,m}$.

$$C_{i,j,m}^{R} \geq \rho_{j,m}^{R}\left(C_{i,m}^{IN} + C_{i,m}^{P}\right) - V_{i,j,m}\sigma_{j,m}^{1}, \; i, \; j, \; m \tag{32}$$

$$C_{i,j,m}^{R} \geq \theta_{j,m}^{R} X_{i,j,m} - \left(1 - V_{i,j,m}\right)\sigma_{j,m}^{2}, \; i, \; j, \; m \tag{33}$$

where $\sigma_{j,m}^{1}$ and $\sigma_{j,m}^{2}$ are big-M parameters.

Variable $C_{i,m}^{IN}$ can be calculated from the individual flows of runoff components between cells, $C_{i,i',m}$,

$$C_{i,m}^{IN} = \sum_{i' \in \mathbf{I}_i^{A} \setminus \mathbf{I}_i^{AL}} C_{i',i,m}, \; i, \; m \tag{34}$$

where $\mathbf{I}_i^{AL}$ is the set of cells i' adjacent to cell i and at a lower elevation.

A given fraction, $\lambda_{i,m}^{I}$, of runoff components flowing into and produced in a cell, less that absorbed by the crop, can infiltrate into the soil depending on the slopes surrounding the cell. The calculation of this parameter is detailed in the Supplementary Material. With this parameter, the amount of runoff components infiltrating into the soil, $C_{i,m}^{I}$ is calculated,

$$C_{i,m}^{I} = \lambda_{i,m}^{I}\left(C_{i,m}^{IN} + C_{i,m}^{P} - \sum_{j} C_{i,j,m}^{R}\right), \; i, \; m \tag{35}$$

We then construct a mass balance requiring the flow of runoff component entering plus the amount being produced within a cell to equal the amount removed and flowing out of the cell, $C_{i,m}^{OUT}$,

$$C_{i,m}^{IN} + C_{i,m}^{P} = C_{i,m}^{OUT} + \sum_{j} C_{i,j,m}^{R} + C_{i,m}^{I}, \; i, m \tag{36}$$

A fraction, $\lambda_{i,m}^{L}$, of the runoff components infiltrating into the soil will leach, and the remainder is absorbed by the soil,

$$C_{i,m}^{L} = \lambda_{i,m}^{L} C_{i,m}^{I}, \; i, m \tag{37}$$

We assume knowledge of the slopes in the cropland, and therefore of the expected flow of water and runoff components between adjacent cells. We further assume that the flow of runoff components precisely follows the flow of water. Parameter $\lambda_{i,i'}$ indicates the fraction of runoff components flowing out of cell i that would flow to adjacent cell i' at a lower elevation to calculate the flow of runoff components between cells. Parameter $\lambda_{i,i'}$ is calculated with a simplified multiple flow direction method based on (Freeman, 1991), with flow allocated proportionally to the slope relative to the sum of the slopes between the cell and all adjacent cells at lower elevation, provided in the Supplementary Material.

$$C_{i,i',m} = \lambda_{i,i'} C_{i,m}^{OUT}, \; i, i' \in \mathbf{I}_i^{AL}, m \tag{38}$$

Similarly, we use the fraction of runoff components out of a cell that exits the cropland, λ_i^{O}, to calculate the total amount of runoff components exiting the cropland from a cell, C_i^{O},

$$C_{i,m}^{O} = \lambda_i^{O} C_{i,m}^{OUT}, \; i, m \tag{39}$$

2.1.6. *Objective function*

We include relative weights for crop production (ω^{P}), biodiversity

(ω^B), GHG balance (ω^G), and water quality (ω^W). The value of the weight for each objective function is user-defined, depending on the objective function the user wishes to prioritize. The biodiversity objective naturally falls between 0 and 1 and for simplicity in determining appropriate weights, each other objective is normalized using parameters $\xi^{P_1}, \xi^{P_2}, \xi^{G_1}, \xi^{G_2}$, and ξ^W_m such that a value of 1 indicates that objective is the highest it could be, and 0 being the lowest. These parameters are calculated by solving the model four times, maximizing each objective function individually. The normalization parameters are calculated to scale the maximum value for each objective to be 1, and the minimum value for each objective (obtained when the other objectives are maximized) to be 0. In this paper, we maintain weights that sum to 1, in which case the total objective value scales between 0 and 1 because each individual objective is already scaled between 0 and 1. We assume that each species group is weighted equally for the biodiversity objective. However, this could be easily changed by introducing an additional parameter describing the relative importance of a given species group and multiplying it by B_k in the objective function.

$$\begin{aligned} Max\ Obj \quad &= \omega^P \xi^{P_1}\left(\xi^{P_2} + R\right) + \frac{\omega^B}{|\mathbf{K}|}\sum_k B_k + \omega^G \xi^{G_1}\left(\xi^{G_2} - \sum_i G_i\right) \\ &\quad + \omega^W \sum_{i,m}\left(1 - \frac{C^O_{i,m} + C^L_{i,m}}{\xi^W_m}\right) \end{aligned} \tag{40}$$

We note that for a given patch, there are many symmetric solutions involving different cells being the sink for the patch. Furthermore, there are symmetric solutions involving breaking a larger patch into smaller patches that are connected to each other if each smaller patch is still larger than the critical area requirement for all species groups. Therefore, to reduce the number of symmetric solutions and improve solution time, we add a penalty term ϵ^F for flows that go up or to the right ($i, i' \in \mathbf{I}^{UR}_i$) and a penalty term ϵ^Z for the number of patches to the objective function,

$$\begin{aligned} Max\ Obj \quad &= \omega^P \xi^{P_1}\left(\xi^{P_2} + R\right) + \frac{\omega^B}{|\mathbf{K}|}\sum_k B_k + \omega^G \xi^{G_1}\left(\xi^{G_2} - \sum_i G_i\right) \\ &\quad + \omega^W \sum_{i,m}\left(1 - \frac{C^O_{i,m} + C^L_{i,m}}{\xi^W_m}\right) - \epsilon^F \sum_{i,i' \in \mathbf{I}^{UR}_i, j} F_{i,i',j} - \epsilon^Z \sum_{i,j} Z_{i,j} \end{aligned} \tag{41}$$

We provide representative examples for how these penalty terms and redundant constraints improve the solution time in the Supplementary Material.

2.2. Edge impacts

We explore different options for including the impact of edges. One option is to assume that only core area, or area of a patch sufficiently far from the edges of a patch such that it is not affected by those edges, contributes to biodiversity. However, not all species groups studied may be impacted by edges in the same way. Depending on the species group considered, the location, and the type of crops, edges can have either a positive or negative effect on biodiversity. For example, researchers have found that increased edges can decrease the species richness of species groups such as beetles, butterflies, ants, and some types of birds (Haddad et al., 2015). However, other researchers have found that higher edge length can actually increase the species richness of birds (Terraube et al., 2016). Therefore, an alternative is to model edges between different pairs of crops as having potentially different impacts (e.g. edges between one pair of crops increase biodiversity, but edges between a different pair of crops decrease biodiversity).

2.2.1. Core area

In this section, we use the concept of core area to denote cells that are within a patch, rather than those on the perimeter of a patch (rooks-case). Binary variable $U_{i,j}$ is used to indicate if cell i with crop j is a core cell.

First, if there are pre-specified crop establishment decisions, some information on core area will already be known for cells with those establishment decisions and for adjacent cells. The combination of cells and crops for which core area is already known is represented as $\mathbf{I}^{FU}_j$. For these combinations of cells and crops, we fix $U_{i,j}$ to its pre-determined value $\tau_{i,j}$,

$$U_{i,j} = \tau_{i,j},\ i \in \mathbf{I}^{FU}_j,\ j \tag{42}$$

For the remaining cells, $U_{i,j}$ is activated by the following equations,

$$U_{i,j} \le X_{i,j},\ i \in \mathbf{I}\backslash\mathbf{I}^{FU}_j,\ j \tag{43}$$

$$U_{i,j} \le X_{i',j},\ i \in \mathbf{I}\backslash\mathbf{I}^{FU}_j,\ i' \in \mathbf{I}^A_i,\ j \tag{44}$$

We note that because core area is always beneficial, we do not need another equation forcing $U_{i,j}$ to be 1.

When only cells that are core area contribute to flows, a tighter upper bound on flows, δ^U_j can be calculated. A cell cannot be core area for a crop if it is on the edge of the cropland ($i \in \mathbf{I}^E$) or is on the interior of the cropland but is adjacent to a cell pre-specified to have a different crop established,

$$\delta^U_j = |\mathbf{I}| - \sum_{i \in \mathbf{I}\backslash\mathbf{I}^E} \max_{i' \in \mathbf{I}^A_i, j', j' \neq j} \chi_{i',j'} - \left|\mathbf{I}^E\right|,\ j \tag{45}$$

where $\mathbf{I}^E$ is the set of cells on the edge of the field. By substituting $U_{i,j}$ in place of $X_{i,j}$ and using the new upper bound δ^U_j in Eqs. (4)–(6) and (8)–(10), only core cells will count as area towards supporting biodiversity,

$$\sum_{i' \in \mathbf{I}^A_i} F_{i,i',j} \le \left(\delta^U_j - 1\right) U_{i,j},\ i,\ j \tag{46}$$

$$Z_{i,j} \le U_{i,j},\ i,\ j \tag{47}$$

$$\sum_{i' \in \mathbf{I}^A_i} F_{i,i',j} - \sum_{i' \in \mathbf{I}^A_i} F_{i',i,j} = U_{i,j} - F^{SINK}_{i,j},\ i,\ j \tag{48}$$

$$F^{SINK}_{i,j} \le \delta^U_j Z_{i,j},\ i,\ j \tag{49}$$

$$\widehat{F}^{SINK}_{i,j} \le \delta^U_j \left(1 - Z_{i,j}\right),\ i,\ j \tag{50}$$

$$\sum_i F^{SINK}_{i,j} = \sum_i U_{i,j},\ j \tag{51}$$

2.2.2. Edge binary variables

Next, to model the impact that edges between different crops may have on each objective, we introduce a binary variable $Y_{i,i',j,j'}$ to indicate if adjacent cells i and i' have crops j and j', respectively. Because the same edge can be referenced in either direction ($Y_{i,i',j,j'} = Y_{i',i,j',j}$), the equations activating $Y_{i,i',j,j'}$ need only be written in one direction, chosen to be up and to the right from cell i ($i' \in \mathbf{I}^{UR}_i$). Similar to the previous section, based on potential pre-specified crop establishment decisions, the value of $Y_{i,i',j,j'}$ will be pre-determined as $\gamma_{i,i',j,j'}$ for set $\mathbf{J}^{FY}_{i,i',j'}$,

$$Y_{i,i',j,j'} = \gamma_{i,i',j,j'},\ i,\ i' \in \mathbf{I}^{UR}_i,\ j \in \mathbf{J}^{FY}_{i,i',j'}, j' \tag{52}$$

Eq. (53) enforces that for an edge between cells i and i' and crop j, $Y_{i,i',j,j'}$ can only be 1 if crop j is planted in cell i. Eq. (54) enforces the same, but for crop j' being planted in an adjacent cell i'.

$$\sum_{j', j' \neq j} Y_{i,i',j,j'} \le X_{i,j},\ i,\ i' \in \mathbf{I}^{UR}_i,\ j \tag{53}$$

$$\sum_{j,j\neq j'} Y_{i,i',j,j'} \leq X_{i',j'},\ i,\ i' \in \mathbf{I}_i^{UR},\ j' \tag{54}$$

To enforce that $Y_{i,i',j,j'}$ is activated, the following equation is introduced,

$$Y_{i,i',j,j'} \geq X_{i,j} + X_{i',j'} - 1,\ i,\ i' \in \mathbf{I}_i^{UR},\ j,\ j',j' \neq j \tag{55}$$

We note that there are several different possible formulations to activate $Y_{i,i',j,j'}$. Eqs. (53) and (54) could be formulated as equalities, or written for all $i,\ i',j$, and j' rather than summing over j'. However, we found empirically that formulating them as presented herein resulted in the fastest solution times.

2.2.3. Edge impact on biodiversity

Here we reformulate the equations for flows to include flow adjustments from edges. These flow adjustments change the effective area of the patch, thereby converting the presence of an edge into a change in area based on the type of edge. Because an edge between two crops could have a different effect for different species groups, flows between cells are also indexed by species group ($F^E_{i,i',j,k}$). This requires reformulation of many of the equations for flows. First, Eq. (6) is reformulated to include flows due to edges,

$$\sum_{i' \in \mathbf{I}_i^A} F^E_{i,i',j,k} - \sum_{i' \in \mathbf{I}_i^A} F^E_{i',i,j,k} = X_{i,j} + \sum_{i' \in \mathbf{I}_i^{UR},j',j' \neq j} \eta^E_{j,j',k} Y_{i,i',j,j'} + \sum_{i' \in \mathbf{I}_i^{UR},j',j' \neq j} \eta^E_{j,j',k} Y_{i',i,j',j} - F^{ESINK}_{i,j,k},\ i,\ j,\ k \tag{56}$$

where $F^{ESINK}_{i,j,k}$ is the flow into a sink at cell i for a patch of crop j for species group k and $\eta^E_{j,j',k}$ is the impact of an edge between two different crops on the total effective area of a species group. Other than flows now being indexed by species group, the difference from Eq. (6) is the two terms including summations of $\eta^E_{j,j',k} Y_{i,i',j,j'}$, which add additional flows if $\eta_{j,j',k} > 0$ (or reduce existing flows if $\eta_{j,j',k} < 0$). Parameter $\eta^E_{j,j',k}$ can vary based on the local conditions of the cropland and species of interest, and therefore would need to be parameterized accordingly. In the present work, we explore representative values corresponding to two cases: (1) a patch consisting of only one cell would not contribute at all to biodiversity of a species group ($\eta^E_{j,j',k} = -0.25$), and (2) when the benefit from edges of a patch of a single cell matches the benefit from its area ($\eta^E_{j,j',k} = 0.25$).

In this case, the upper bound on flows must be updated from Eq. (3) to consider the potential impact of edges. For a given combination of crop and species group, $\delta^E_{j,k}$ includes the impact of edges known to be present based on pre-specified crop establishment decisions,

$$\delta^E_{j,k} = |\mathbf{I}| + \sum_{i \in \mathbf{I}_j^{FX},i' \in \mathbf{I}_i^A \cap \mathbf{I}_{j'}^{FX},j',j' \neq j} \frac{\eta^E_{j,j',k}}{2} - \sum_{i' \in \mathbf{I}_{j'}^{FX},j',j' \neq j} \chi_{i',j'},\ j,\ k \tag{57}$$

We note that this upper bound is valid if planting a crop in a cell is more beneficial than the sum of all edge effects ($\eta_{j,j',k} \leq 0.25$). If that is not the case, a larger upper bound must be used, which is presented as Equation S25 in the Supplementary Material. Eqs. (4) and (7)–(10) must also be reformulated with flows being indexed by species group,

$$\sum_{i' \in \mathbf{I}_i^A} F^E_{i,i',j,k} \leq \left(\delta^E_{j,k} - 1\right) X_{i,j},\ i,\ j,k \tag{58}$$

$$\sum_{i' \in \mathbf{I}_i^A} F_{i',i,j,k} + Z_{i,j} = F^{ESINK}_{i,j,k} + \widehat{F}^{ESINK}_{i,j,k},\ i,\ j,k \tag{59}$$

$$F^{ESINK}_{i,j,k} \leq \delta^E_{j,k} Z_{i,j},\ i,\ j,k \tag{60}$$

$$\widehat{F}^{ESINK}_{i,j,k} \leq \left(\delta^E_{j,k} - 1\right)\left(1 - Z_{i,j}\right),\ i,\ j,k \tag{61}$$

$$\sum_i F^{SINK}_{i,j,k} = \sum_i X_{i,j} + \sum_{i' \in \mathbf{I}_i^{UR},j',j' \neq j} \eta^E_{j,j',k} Y_{i,i',j,j'} + \sum_{i' \in \mathbf{I}_i^{UR},j',j' \neq j} \eta^E_{j,j',k} Y_{i',i,j',j},\ j,\ k \tag{62}$$

where $\widehat{F}^{ESINK}_{i,j,k}$ is a dummy variable for flows into cells that are not sinks.

The effective area is then calculated based on the new variable for flow into sinks and the upper bound on flows is updated,

$$\alpha F^{ESINK}_{i,j,k} = A^{EFF}_{i,j,k} + \widehat{A}^{EFF}_{i,j,k},\ i,j,k \tag{63}$$

$$\zeta_{j,k} W_{i,j,k} \leq A^{EFF}_{i,j,k} \leq \alpha \delta^E_{j,k} W_{i,j,k},\ i,j,k \tag{64}$$

We also update the flow penalty term in the objective function with the new flow variable,

$$Obj = \omega^P \xi^{P_1}\left(\xi^{P_2} + R\right) + \frac{\omega^B}{|\mathbf{K}|}\sum_k B_k + \omega^G \xi^{G_1}\left(\xi^{G_2} - \sum_i G_i\right) + \omega^W \sum_{i,m}\left(1 - \frac{C^O_{i,m} + C^L_{i,m}}{\xi^W_m}\right) - \epsilon^F \sum_{i,i' \in \mathbf{I}_i^{UR},j,k} F^E_{i,i',j,k} - \epsilon^Z \sum_{i,j} Z_{i,j} \tag{65}$$

3. Results

To demonstrate the model, we apply it to a 19-hectare field that is part of the Great Lakes Bioenergy Research Center (GLBRC) Scale-up Experiment at Marshall Farms, Michigan, USA, for which corn yields in each cell over multiple years are known. We use the average yield of each cell over the years of available data. We estimate the yield of other crops in this field based on their yields in nearby fields and their correlation to corn yields, detailed in the Supplementary Material. We partition the field into 20 × 20 meter cells. For biodiversity, we use data from the nearby GLBRC Bioenergy Cropping System Experiment, which included the number of species of butterflies, bees, and ants found in different bioenergy crops (Haan et al., 2023). Additional parameters are taken from the literature and are detailed in Tables S1-S4 in the Supplementary Material. In all cases, the models are solved with Gurobi 11.0.0 through GAMS 45.4.0 on a PC with a 3.0 GHz Intel Core i5–8500 processor.

3.1. No edge impacts

First, we examine the case of three species groups (ants, bees, and butterflies) and three potential crops to be planted (corn, switchgrass, and reconstructed prairie). We assume that bees have a critical area of 0.2 ha (5 cells), and that ants and butterflies have a critical area less than one cell. This does not necessarily reflect the biology of these groups but is useful as a hypothetical. The model consists of Eqs. (1)–(19), (21)–(39), and (41), resulting in 78,090 equations and 65,235 variables, of which 55,218 are continuous and 10,017 are binary.

We demonstrate the application of the model using the weighted-objective approach to create a pareto front, shown in Fig. 4. Here, we combine the biodiversity, GHG sequestration, and water quality objectives into one environmental objective, each scaled to contribute equally to the combined objective. The pareto front shows how significant increases in the combined environmental objective (up to around 0.5) can be achieved with a negligible reduction in the profit. Further increasing the combined environmental objective, however, can lead to significant reductions in profit. A further set of example results examining the impact of varying the weights between biodiversity and the other environmental objective functions is provided in the Supplementary Material.

Next, we solve the model optimizing only one objective. For some objectives, solutions with the same value in the primary objective but different values for the other objectives can be obtained. For example, when biodiversity is maximized, the same total area of each crop can be planted in different configurations, or with different amounts of

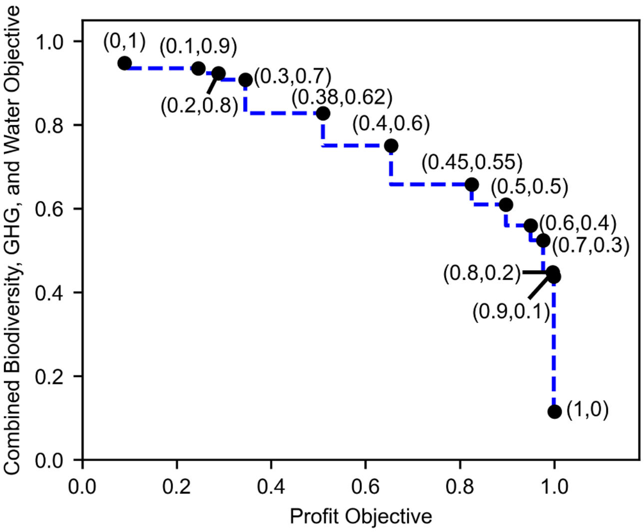

Fig. 4. Pareto front of profit and combined biodiversity, GHG sequestration, and water quality objectives. Results are obtained using a weighted-objective approach, with labels on each data point indicating the objective weight for profit and the combined environmental objectives, respectively.

fertilization, that can lead to different values for the other objectives without changing the biodiversity objective. When this is the case, after solving the model using the primary objective, we then solve the model again using a secondary objective without permitting a reduction in the first objective. Each instance is solved to a 0.1 % optimality gap within 4 hours. In Fig. 5, we show example optimal layouts and objective values for several instances of different orders of sequential optimization. An example of the model without edge impacts solved using the weighted objective method is given in the Supplementary Material.

When corn is planted in all cells and has the maximum amount of fertilizer applied (Fertilized Corn), there are some cells with very low corn yield that have a negative profit. When profit is maximized (P, shown in Fig. 5b), switchgrass is planted in these cells because the lower cost of management of switchgrass and the option to not fertilize these cells can increase profit. The addition of switchgrass and the reduction in fertilizer application also causes increases in biodiversity, GHG sequestration, and water quality.

When GHG sequestration is maximized (G), prairie is planted in the entire field and is fertilized to increase soil organic carbon sequestration, which more than offsets the emissions from fertilizer production and increased NO_x emissions. This results in a relatively high water quality objective, but not the maximum possible due to the fertilizer application. The biodiversity score is not at the maximum because only one crop is present.

When water quality is maximized, corn is not planted because of the addition of pesticides with the corn crop. If profit is maximized next after water quality (WP), switchgrass is planted everywhere. If instead biodiversity is maximized after water quality (WB), a combination of switchgrass and prairie is chosen to achieve near the maximum biodiversity score possible.

Because we assume biodiversity is only affected by the area of each crop planted, there are many designs that could result in the maximum biodiversity score possible. When profit is maximized second (BP, shown in Fig. 5a), corn is planted in the highest-yielding areas and fertilized, while prairie and switchgrass are planted in lower-yielding areas and not fertilized. If GHG sequestration is maximized second (BG), the fertilization decisions are reversed: prairie and switchgrass are fertilized, and corn is not. Finally, if water quality is maximized second (BW), no crops are fertilized.

3.2. Biodiversity edge impacts

We examine the case of three species groups (ants, bees, and butterflies) and two potential crops to be planted (corn and switchgrass). We assume that all species have a critical area of 0.2 ha (5 cells). We solve the model with different treatment of edges and show the resulting optimal cropland design in Fig. 6. We assume that cells which have reliable high yield over many years (high stable yield, cells with black borders in Fig. 6), are pre-specified to have corn planted.

When no edge impacts are considered, the model is the same as in the

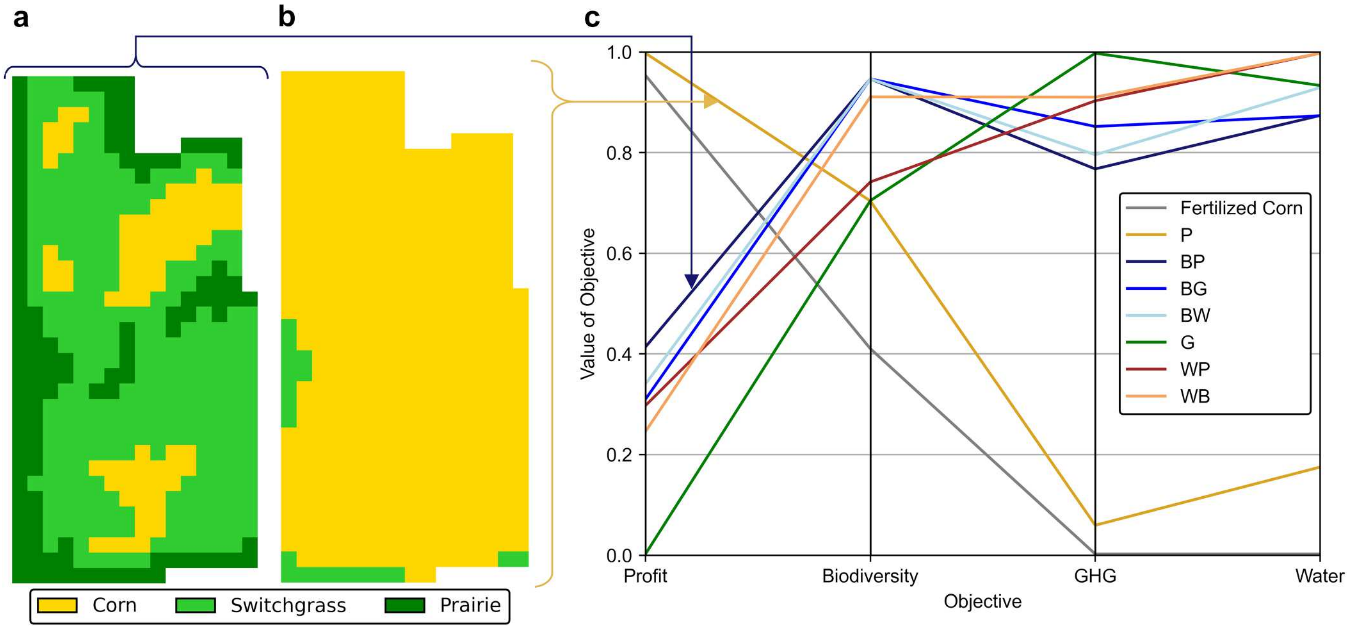

Fig. 5. Optimal cropland layout when biodiversity is maximized first then profit is maximized (a), optimal cropland layout when profit is maximized (b), value of each objective for different primary and secondary objectives (c). The naming convention for each line in (c) is the first letter of the name of objective given in the order in which objectives are maximized (B: biodiversity, G: GHG sequestration, P: profit, W: water quality). The only exception to this convention is 'Fertilized Corn', in which it is pre-specified that corn be planted in all cells and fertilized at the maximum allowable amount.

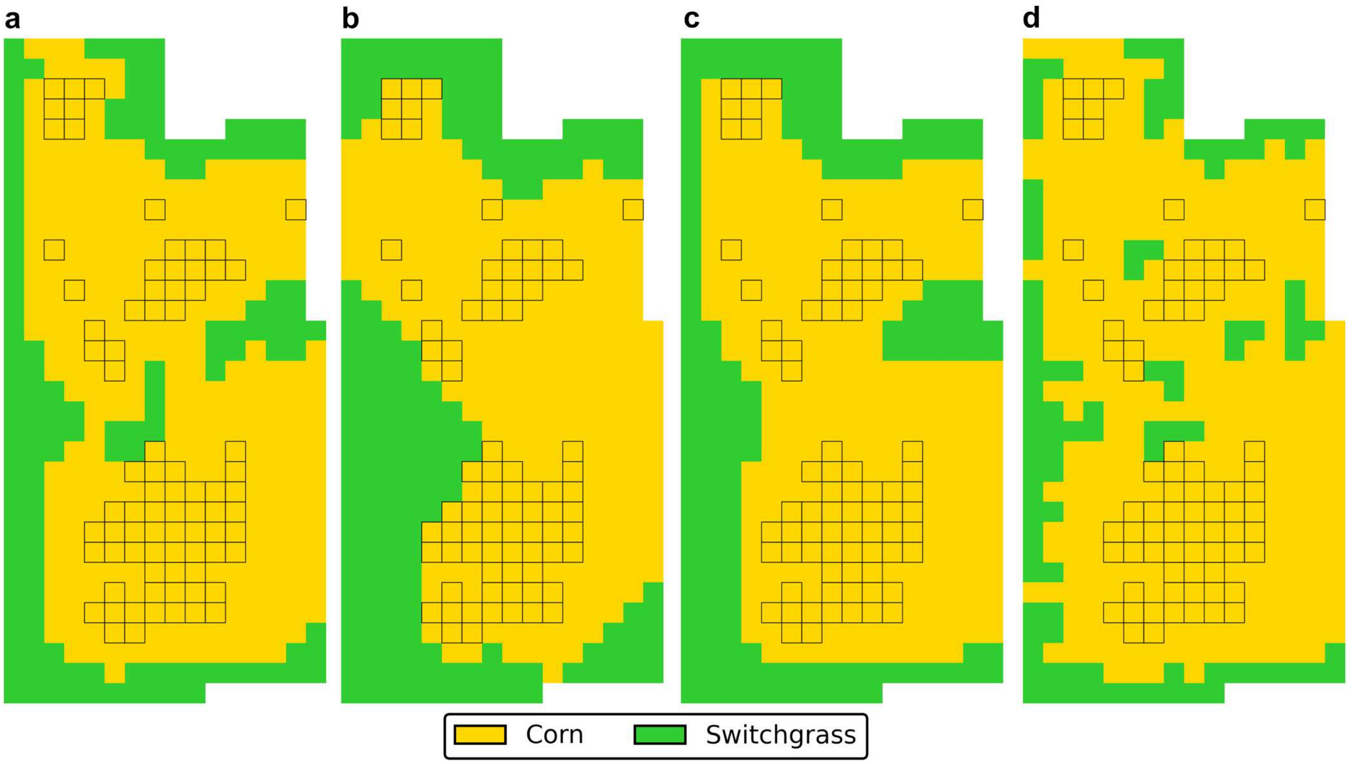

Fig. 6. Optimal cropland design for when (a) edges have no effect on biodiversity, (b) only core area contributes to biodiversity, (c) edges decrease biodiversity ($\eta_{j,j',k} = -0.25$ for the edge between switchgrass and corn for all species groups), (d) edges increase biodiversity ($\eta_{j,j',k} = 0.25$ for the edge between switchgrass and corn for all species groups). All instances are solved with objective weights of 0.1, 0.9, 0, and 0 for profit, biodiversity, GHG sequestration, and water quality, respectively. In all instances, cells with high stable yield of corn (those with black borders) are pre-specified to have corn established.

previous section. When explicit edge impacts are considered, the model consists of Eqs. (1), (2), (5), (13), (14), (16)–(20), (21)–(39), and (52)–(65). When only core area counts towards biodiversity, the model consists of Eqs. (1), (2), (7), (11)-(20), (21)–(39), and (41)–(51).

When no edge impacts are considered (Fig. 6a), switchgrass is planted in four patches consisting of the cells with the lowest yield, similarly to where prairie was planted in Fig. 5a. When only core area benefits biodiversity (Fig. 6b), only three patches of prairie appear, and those patches are much more compact than in Fig. 6a. When edges decrease biodiversity (Fig. 6c), only two patches of prairie are selected. In contrast to when only core area contributes to biodiversity, when edges decrease biodiversity, narrow rows of switchgrass are still beneficial for biodiversity. Lastly, when edges increase biodiversity (Fig. 6d), eleven small patches of switchgrass are planted to maximize edges at the expense of larger patches. Because $\eta_{j,j',k} = 0.25$ for all species groups, even a patch with only three cells and eight edges meets the critical area requirement for all species. We note that this cropland layout may not be realistically implemented but shows a potential layout in the extreme case where edges benefit all species groups and where ease of harvesting is not an issue.

4. Discussion and conclusions

4.1. Contributions

We proposed a MIQCP model to aid design of cropland establishment and fertilizer decision-making while balancing profit, biodiversity, GHG balance, and water quality objectives. The model estimates the biodiversity of the cropland based on the area of each crop and species-area curves for each combination of species group and plant type. Water quality and GHG sequestration is calculated based on crop establishment and fertilization decisions. Further, the model supports the consideration of edge impacts by only counting core area towards biodiversity, or by an explicit positive or negative effect for each combination of edge and species group.

4.2. Limitations and future work

In this paper, we presented examples for different combinations of weights in the objective function, but the same model can be solved in different ways to answer different questions. For example, a decision maker may be interested in the cropland design that results in the maximum biodiversity score with no more than a specified reduction in profit. Such an analysis could be performed with only minimal changes in the model.

While our case study results demonstrate a simple application using representative variables at the level of an individual field, the proposed model and approach can be expanded and extended to several additional application areas. First, the flexible nature of our multi-objective MIQCP model would allow for the integration of additional objectives such as water use, vegetation quality, drought susceptibility, labor intensity, or pest predation. Second, the model could be used to aid planning and landscape design at multiple scales. For example, at the level of individual farms, producers could use the model to estimate the optimal design among multiple fields, seeking to balance crop types and objective across their entire operation. At a coarser resolution, the model could be adapted to consider larger scales (e.g., regional) and include additional elements such as supply chain design of the biomass transportation to final markets.

Our model could also be adapted or scaled to achieve additional goals without structurally adding new constraints. For example, the side length of each cell could be set to match the size of the equipment used on the cropland, such that the resolution of the model matches real world constraints. The model's unit of analysis could also be shifted from cell-based to polygon based to match existing landscape features, though this would require reformulation of several equations in the model presented such as those tracking the area of patches and the impact of edges.

Depending on the total number of cells or features in the cropland and how edges or interactions are considered, the model may become computationally expensive. In such cases, solving the model first at a finer resolution and using the solution as a warm start for the model at a finer resolution can be helpful. Beyond that, tailored solution methods, potentially based on decomposing the field into smaller subfields, may become necessary for particularly large instances. The model presented also assumes that harvesting costs are only a function of crop establishment and fertilization decisions. Further research could estimate the cost of harvesting based on the layout of crops, though that would inherently make the model more computationally demanding to solve. Alternative formulations for estimating the fraction of species within a group that would be present in the cropland, such as using logarithmic functions instead of a series of quadratic equations, could also be explored.

As tracking the definite presence of individual species is not possible in an optimization model designing a cropland, we used a probabilistic estimate of biodiversity based on the predicted presence of species in each crop type. These assumptions neglect the complex dynamics of species distribution that cannot be readily modeled. Getting accurate results thus depends on the quality of data, some of which is not easy to obtain. However, remote sensing and integration of experiments with biodiversity quantification and modeling could aid in obtaining realistic parametrizations for any cropland of interest.

We note that to make the model tractable, we use a simplified hydrological model and a uniform soil system. For example, we assume runoff as a fixed fraction of precipitation and do not calculate the flow of runoff components on daily time steps with soil moisture conditions in space. These assumptions reduce the spatial heterogeneity of water quality sources and sinks. The related dynamics of soil organic carbon and NO_x are similarly simplified. Including more realistic spatial heterogeneity could identify additional spatial tradeoffs related to profit, water quality, and GHG emissions. Future research can couple the general optimization model with a more detailed hydrologic and crop-soil system model, potentially unique to each yield stability zone for a given cropland of interest. The inclusion of a temporal dimension could also allow for additional consideration of time-dependent variables such as crop rotations.

4.3. Conclusions

The developed model allows us to demonstrate the benefits that carefully designed cultivated landscapes can provide. For example, in the case study that we examine there are clear tradeoffs between maximizing profit versus the environmental objectives. Planting switchgrass or prairie in place of corn increases biodiversity, GHG sequestration, and water quality simultaneously, though by different amounts and with potentially large negative impacts on profit. However, there are solutions where switchgrass is planted in areas with low corn yield that are better than planting and fertilizing corn in all cells (the status quo) for each of the four objectives (Basso & Antle, 2020). The presented model demonstrates the importance of measuring and optimizing multiple objectives at the sub-field, field, and landscape scale to achieve better outcomes for all competing objectives. The precise values for these objectives and the benefits of planting perennial vegetation in croplands will depend heavily on field-specific data such as soil, weather conditions, yields, and input rates. High-quality data, such as from remote sensing images, tractor-based yield, and input monitoring, and simulations from distributed models for the estimates of hard/expensive to measure values (i.e., soil organic carbon, NO_x, and runoff component fluxes) will be critical for real-world application.

Nomenclature

Sets

$\mathbf{I}$	Cells
$\mathbf{J}$	Crops
$\mathbf{K}$	Species groups
$\mathbf{L}$	Set of linear approximation segments for species-area curve
$\mathbf{M}$	Set of runoff components

Subsets

$\mathbf{I}_{i'}^{A}$	Cells i that are adjacent to cell i'
$\mathbf{I}_{i'}^{AL}$	Cells i that are adjacent to cell i' and at lower elevation
$\mathbf{I}^{E}$	Cells i that are on the edge of the cropland
$\mathbf{I}_{j}^{FX}$	Cells i that have a pre-specified crop establishment decision for crop j
$\mathbf{I}_{j}^{FU}$	Cells i that have a pre-specified crop core area decision for crop j
$\mathbf{I}_{i'}^{UR}$	Cells i that are adjacent above or to the right of cell i'
$\mathbf{J}^{C}$	Crops that are harvested
$\mathbf{J}^{F}$	Singleton subset of the first crop in the set
$\mathbf{J}_{i,i',j'}^{FY}$	Edges between crops j and j' in cells i and i' that have a pre-determined edge decision
$\mathbf{J}^{L}$	Singleton subset of the last crop in the set
$\mathbf{M}^{N}$	Singleton subset of nitrogen

Parameters

α	Area of a cell
$\beta_{i,j}^{F}$	Upper bound on fertilizer application to crop j in cell i
$\gamma_{i,i',j,j'}$	Pre-specified decision for an edge between adjacent cells i and i' with crops j and j' based on the prespecified crop decision $\chi_{i,j}$
$\zeta_{j,k}$	Critical area for species k
$\delta_j / \delta_j^U / \delta_{j,k}^E$	Upper bound on flows for crop j
ϵ^F / ϵ^Z	Penalty for flows/number of sinks
$\eta_{j,j',k}^{E}$	Adjustment to area for species k due to edge between crops j and j'
$\theta_{j,m}^{R}$	Upper bound on runoff component m removal by one cell of crop j
$\kappa_{j,m}^{N}$	Amount of runoff component m added by fertilizer to crop j
$\kappa_{j,m}^{P}$	Amount of runoff component m produced by crop j
$\lambda_{i,i'}$	Fraction of runoff component exiting cell i that flows to cell i'
$\lambda_{i,m}^{I}$	Fraction of runoff component m entering cell i that infiltrates the soil
$\lambda_{i,m}^{L}$	Fraction of runoff component m infiltrating the soil in cell i that leaches
λ_{i}^{O}	Fraction of runoff components exiting cell i that flows out of cropland
$\mu_{j,k,l}^{1} / \mu_{j,k,l}^{2}$	Parameters for linear approximation of species-area curve
$\xi^{G_1} / \xi^{G_2} / \xi^{P_1} / \xi^{P_2} / \xi_m^W$	Scaling parameter for greenhouse gas balance/production/ water quality objectives
$\pi_{i,j}^{C}$	Total cost of planting and harvesting crop j in cell i
π^{N}	Price of purchasing and applying fertilizer
π_{j}^{S}	Selling price of crop j
$\rho_{j,m}^{R}$	Fraction of runoff component m removed by crop j
$\sigma_{j,m}^{1} / \sigma_{j,m}^{2}$	Big-M values for runoff component removal
$\tau_{i,j}$	Pre-specified decision for cell i being core area for crop j based on the pre-specified crop decision $\chi_{i,j}$
$\phi_{i,j}^{C}$	Baseline greenhouse gas emissions from crop j in cell i (sum of planting, harvesting, soil organic carbon sequestration)
$\phi_{i,j}^{E}$	Change in greenhouse gas emissions if fertilizer is applied
ϕ^{F}	Greenhouse gas emissions from fertilizer
$\chi_{i,j}$	Pre-specified binary decision for the establishment of crop j in cell i
$\psi_{i,j}$	Yield of crop j in cell i
$\psi_{i,j}^{F}$	Additional yield of crop j in cell i per unit of fertilizer applied
$\omega^B / \omega^G / \omega^P / \omega^W$	Weight in objective for biodiversity/greenhouse gas balance/ production/water quality

Binary Variables

$U_{i,j}$	1 if cell i is core area for crop j

(*continued on next page*)

(*continued*)

$V_{i,j,m}$	1 if runoff component m removal by crop j in cell i is limited by the upper bound
$W_{i,j,k}$	1 if patch with sink at cell i is large enough to support species k
$X_{i,j}$	1 if crop j is established in cell i
$Y_{i,i',j,j'}$	1 if adjacent cells i and i' have crop j and j'
$Z_{i,j}$	1 if cell i is a sink for crop j

Nonnegative Continuous Variables

$A^{EFF}_{i,j,k}$	Effective area for species k in patch of crop j with sink at cell i
$\widehat{A}^{EFF}_{i,j,k}$	Dummy variable for effective area for species k in patch of crop j with sink at cell i
$A^{TOT}_{j,k}$	Total effective area of crop j for species k
$\widetilde{A}^{TOT}_{j,k,l}$	Disaggregation of total effective area of crop j for species k in interval l
$B_{j,k}$	Fraction of species in species group k present in crop j
$\widehat{B}_{j,k}$	Dummy variable for fraction of species in species group k present in crop j
B^{TOT}_{k}	Fraction of species in species group k present in the cropland
$C_{i,i',m}$	Flow of runoff component m from cell i to cell i'
$C^{I}_{i,m}$	Amount of runoff component m infiltrating into the soil in cell i
$C^{IN}_{i,m}$	Flow of runoff component m into cell i
$C^{L}_{i,m}$	Amount of runoff component m leaching in cell i
$C^{O}_{i,m}$	Flow of runoff component m exiting the cropland from cell i
$C^{OUT}_{i,m}$	Flow of runoff component m out of cell i
$C^{P}_{i,m}$	Amount of runoff component m produced in cell i
$C^{R}_{i,j,m}$	Amount of runoff component m removed by crop j in cell i
$C_{i,i',m}$	Flow of runoff component m from cell i to cell i'
$F_{i,i',j}$	Flow from cell i to i' for crop j
$F^{E}_{i,i',j,k}$	Flow from cell i to i' for crop j and species group k when edge impacts are included
$F^{ESINK}_{i,j,k}$	Flow into cell i for crop j and species group k if cell i is a sink for crop j and species group k when edge impacts are included
$\widehat{F}^{ESINK}_{i,j,k}$	Dummy variable for flow into cells that are not sinks for crop j and species group k when edge impacts are included
$F^{SINK}_{i,j}$	Flow into cell i for crop j if cell i is a sink for crop j
$\widehat{F}^{SINK}_{i,j}$	Dummy variable for flow into cells that are not sinks for crop j
$N_{i,j}$	Fertilizer applied to crop j in cell i
$P_{i,j}$	Production of crop j in cell i

Continuous Variables

G_i	Greenhouse gas balance in cell i
R	Total profit of the cropland

CRediT authorship contribution statement

Caleb H. Geissler: Writing – review & editing, Writing – original draft, Visualization, Software, Methodology, Formal analysis, Data curation, Conceptualization. **Nathan L. Haan:** Writing – review & editing, Data curation, Conceptualization. **Bruno Basso:** Writing – review & editing, Conceptualization. **Ames Fowler:** Writing – review & editing, Data curation, Conceptualization. **Douglas A. Landis:** Writing – review & editing, Conceptualization. **Tyler J. Lark:** Writing – review & editing, Conceptualization. **Christos T. Maravelias:** Writing – review & editing, Supervision, Project administration, Methodology, Funding acquisition, Conceptualization.

Declaration of competing interest

The authors declare that they have no known competing financial interests or personal relationships that could have appeared to influence the work reported in this paper.

Acknowledgments

This material is based upon work supported by the Great Lakes Bioenergy Research Center, U.S. Department of Energy, Office of Science, Biological and Environmental Research Program under Award Number DE-SC0018409.

Support for this research was provided by the National Science Foundation Long-term Ecological Research Program (DEB 2224712) at the Kellogg Biological Station, and by Michigan State University AgBioResearch.

Supplementary materials

Supplementary material associated with this article can be found, in the online version, at doi:10.1016/j.ecolmodel.2024.110954.

Data availability

Data will be made available on request.

References

Adams, V.M., Pressey, R.L., Álvarez-Romero, J.G., 2016. Using optimal land-use scenarios to assess trade-offs between conservation, development, and social values. PLoS. One 11 (6), 1–20. https://doi.org/10.1371/journal.pone.0158350.

Ball, I., Possingham, H., 2000. *Marxan* (1.8.2). https://courses.washington.edu/cfr590/software/Marxan1810/marxan_manual_1_8_2.pdf.

Basso, B., 2021. Precision conservation for a changing climate. Nat. Food 2 (5), 322–323. https://doi.org/10.1038/s43016-021-00283-z.

Basso, B., Antle, J., 2020. Digital agriculture to design sustainable agricultural systems. Nat. Sustain. 3 (4), 254–256. https://doi.org/10.1038/s41893-020-0510-0.

Basso, B., Dumont, B., Maestrini, B., Shcherbak, I., Robertson, G.P., Porter, J.R., Smith, P., Paustian, K., Grace, P.R., Asseng, S., Bassu, S., Biernath, C., Boote, K.J., Cammarano, D., De Sanctis, G., Durand, J.-L., Ewert, F., Gayler, S., Hyndman, D.W., Rosenzweig, C., 2018. Soil organic carbon and nitrogen feedbacks on crop yields under climate change. Agric. Environ. Lett. 3 (1), 1–5. https://doi.org/10.2134/ael2018.05.0026.

Basso, B., Ritchie, J.T., 2015. Simulating crop growth and biogeochemical fluxes in response to land management using the SALUS model. In: Hamilton, S.K., Doll, J.E., Robertson, P.G. (Eds.), The Ecology of Agricultural Landscapes: Long-Term Research On the Path to Sustainability. Oxford University Press, pp. 252–274.

Billionnet, A., 2013. Mathematical optimization ideas for biodiversity conservation. Eur. J. Oper. Res. 231 (3), 514–534. https://doi.org/10.1016/j.ejor.2013.03.025.

Brosi, B.J., Armsworth, P.R., Daily, G.C., 2008. Optimal design of agricultural landscapes for pollination services. Conserv. Lett. 1 (1), 27–36. https://doi.org/10.1111/j.1755-263x.2008.00004.x.

Butchart, S.H.M., Walpole, M., Collen, B., Strient, A.van, Scharlemann, J.P.W., Almond, R.E.A., Baillie, J.E.M., Bomhard, B., Brown, C., Bruno, J., Carpenter, K.E., Carr, G.M., Clanson, J., Chenery, A.M., Csirke, J., Davidson, N.C., Dentener, F., Foster, M., Galli, A., Watson, R., 2010. Global biodiversity: indicators of recent declines. Sci. (1979) 328 (May), 1164–1168. https://doi.org/10.1126/science.1187512.

Camm, J.D., Norman, S.K., Polasky, S., Solow, A.R., 2007. Expected species covered. Oper. Res. 50 (6), 946–955. https://doi.org/10.1287/opre.50.6.946.351.

Freeman, T.G., 1991. Calculating catchment area with divergent flow based on a regular grid. Comput. Geosci. 17 (3), 413–422. https://doi.org/10.1016/0098-3004(91)90048-I.

Haan, N.L., Benucci, G.N.M., Fiser, C.M., Bonito, G., Landis, D.A., 2023. Contrasting effects of bioenergy crops on biodiversity. Sci. Adv. 9 (38), 1–13. https://doi.org/10.1126/SCIADV.ADH7960.

Haddad, N.M., Brudvig, L.A., Clobert, J., Davies, K.F., Gonzalez, A., Holt, R.D., Townshend, J.R., 2015. Habitat fragmentation and its lasting impact on Earth's ecosystems. Sci. Adv. 1 (2), 1–9. https://doi.org/10.1126/sciadv.150005.

He, C., Fang, L., Xiong, X., Fan, F., Li, Y., He, L., Shen, X., Li, S., Ji, C., Zhu, J., 2022. Environmental heterogeneity regulates species-area relationships through the spatial distribution of species. For. Ecosyst. 9. https://doi.org/10.1016/j.fecs.2022.100033.

Houghton, R.A., House, J.I., Pongratz, J., Van Der Werf, G.R., Defries, R.S., Hansen, M.C., Le Quéré, C., Ramankutty, N., 2012. Carbon emissions from land use and land-cover change. Biogeosciences. 9 (12), 5125–5142. https://doi.org/10.5194/bg-9-5125-2012.

Jiao, P., Xu, D., Wang, S., Zhang, T., 2011. Phosphorus loss by surface runoff from agricultural field plots with different cropping systems. Nutr. Cycl. Agroecosyst. 90 (1), 23–32. https://doi.org/10.1007/s10705-010-9409-x.

Karlen, D.L., Cambardella, C.A., Kovar, J.L., Colvin, T.S., 2013. Soil quality response to long-term tillage and crop rotation practices Soil quality response to long-term tillage and crop rotation practices. Soil. Tillage Res. 133, 54–64. https://doi.org/10.1016/j.still.2013.05.013.

Kemmerling, L.R., Rutkoski, C.E., Evans, S.E., Helms, J.A., Cordova-Ortiz, E.S., Smith, J. D., Vázquez Custodio, J.A., Vizza, C., Haddad, N.M., 2022. Prairie Strips and Lower Land Use Intensity Increase Biodiversity and Ecosystem Services. Front. Ecol. Evol. 10 (May), 1–18. https://doi.org/10.3389/fevo.2022.833170.

Kennedy, C.M., Hawthorne, P.L., Miteva, D.A., Baumgarten, L., Sochi, K., Matsumoto, M., Evans, J.S., Polasky, S., Hamel, P., Vieira, E.M., Develey, P.F., Sekercioglu, C.H., Davidson, A.D., Uhlhorn, E.M., Kiesecker, J., 2016. Optimizing land use decision-making to sustain Brazilian agricultural profits, biodiversity and ecosystem services. Biol. Conserv. 204, 221–230. https://doi.org/10.1016/j.biocon.2016.10.039.

Kremen, C., Williams, N.M., Thorp, R.W., 2002. Crop pollination from native bees at risk from agricultural intensification. Proc. Natl. Acad. Sci. u S. a 99 (26), 16812–16816. https://doi.org/10.1073/pnas.262413599.

Law, E.A., Meijaard, E., Bryan, B.A., Mallawaarachchi, T., Koh, L.P., Wilson, K.A., 2015. Better land-use allocation outperforms land sparing and land sharing approaches to conservation in Central Kalimantan, Indonesia. Biol. Conserv. 186, 276–286. https://doi.org/10.1016/j.biocon.2015.03.004.

Margules, C.R., Nicholls, A.O., Pressey, R.L., 1988. Selecting networks of reserves to maximise biological diversity. Biol. Conserv. 43 (1), 63–76. https://doi.org/10.1016/0006-3207(88)90078-X.

Nelson, E., Mendoza, G., Regetz, J., Polasky, S., Tallis, H., Cameron, D.R., Chan, K.M.A., Daily, G.C., Goldstein, J., Kareiva, P.M., Lonsdorf, E., Naidoo, R., Ricketts, T.H., Shaw, M.R., 2009. Modeling multiple ecosystem services, biodiversity conservation, commodity production, and tradeoffs at landscape scales. Front. Ecol. Environ. 7 (1), 4–11. https://doi.org/10.1890/080023.

Olsson, O., Brady, M.V., Stjernman, M., Smith, H.G., 2021. Optimizing species richness in mosaic landscapes: A probabilistic model of species-area relationships. Front. conserv. sci. 2 (September), 1–13. https://doi.org/10.3389/fcosc.2021.703260.

Polasky, S., Nelson, E., Camm, J., Csuti, B., Fackler, P., Lonsdorf, E., Montgomery, C., White, D., Arthur, J., Garber-Yonts, B., Haight, R., Kagan, J., Starfield, A., Tobalske, C., 2008. Where to put things? Spatial land management to sustain biodiversity and economic returns. Biol. Conserv. 141 (6), 1505–1524. https://doi.org/10.1016/j.biocon.2008.03.022.

Polasky, S., Nelson, E., Lonsdorf, E., Fackler, P., Starfield, A., 2005. Conserving species in a working landscape: Land use with biological and economic objectives. Ecol. Appl. 15 (4), 1387–1401. https://doi.org/10.1017/CBO9780511551079.021.

Reino, L., Beja, P., Osborne, P.E., Morgado, R., Fabião, A., Rotenberry, J.T., 2009. Distance to edges, edge contrast and landscape fragmentation: Interactions affecting farmland birds around forest plantations. Biol. Conserv. 142 (4), 824–838. https://doi.org/10.1016/j.biocon.2008.12.011.

Sala, O.E., Chapin, F.S., Armesto, J.J., Berlow, E., Bloomfield, J., Dirzo, R., Huber-Sanwald, E., Huenneke, L.F., Jackson, R.B., Kinzig, A., Leemans, R., Lodge, D.M., Mooney, H.A., Oesterheld, M., Poff, N.L.R., Sykes, M.T., Walker, B.H., Walker, M., Wall, D.H., 2000. Global biodiversity scenarios for the year 2100. Science (1979) 287 (5459), 1770–1774. https://doi.org/10.1126/science.287.5459.1770.

Schlegel, J., 2022. Butterflies benefit from forest edge improvements in Western European lowland forests, irrespective of adjacent meadows' use intensity. For. Ecol. Manage 521 (May), 120413. https://doi.org/10.1016/j.foreco.2022.120413.

Schulte, L.A., Niemi, J., Helmers, M.J., Liebman, M., Arbuckle, J.G., James, D.E., Kolka, R.K., O'Neal, M.E., Tomer, M.D., Tyndall, J.C., Asbjornsen, H., Drobney, P., Neal, J., Van Ryswyk, G., Witte, C., 2017. Prairie strips improve biodiversity and the delivery of multiple ecosystem services from corn–soybean croplands. Proc. Natl. Acad. Sci. u S. a 114 (42), 11247–11252. https://doi.org/10.1073/pnas.1620229114.

Shirabe, T., 2009. Districting modeling with exact contiguity constraints. Environ. Plan. B: Plan. Des. 36 (6), 1053–1066. https://doi.org/10.1068/b34104.

Stanford University, University of Minnesota, Chinese Academy of Sciences, The Nature Conservancy, World Wildlife Fund, Stockholm Resilience Centre, Royal Swedish Academy of Sciences, 2023. *InVEST* (3.14.0). https://naturalcapitalproject.stanford.edu/software/invest.

Strassburg, B.B.N., Beyer, H.L., Crouzeilles, R., Iribarrem, A., Barros, F., de Siqueira, M. F., Sánchez-Tapia, A., Balmford, A., Sansevero, J.B.B., Brancalion, P.H.S., Broadbent, E.N., Chazdon, R.L., Filho, A.O., Gardner, T.A., Gordon, A., Latawiec, A., Loyola, R., Metzger, J.P., Mills, M., Uriarte, M., 2019. Strategic approaches to restoring ecosystems can triple conservation gains and halve costs. Nat. Ecol. Evol. 3 (1), 62–70. https://doi.org/10.1038/s41559-018-0743-8.

Terraube, J., Archaux, F., Deconchat, M., van Halder, I., Jactel, H., Barbaro, L., 2016. Forest edges have high conservation value for bird communities in mosaic landscapes. Ecol. Evol. 6 (15), 5178–5189. https://doi.org/10.1002/ece3.2273.

Tilman, D., Hill, J., Lehman, C., 2006. Carbon-negative biofuels from low-input high-diversity grassland biomass. Sci. (1979) 314 (5805), 1598–1600. https://doi.org/10.1126/science.1133306.

U.S. Bioenergy Statistics, 2024. Bioenergy Statistics. https://www.ers.usda.gov/data-products/u-s-bioenergy-statistics/.

Vallejos, L.M., Prevedello, J.A., Vecchi, M.B., Alves, M.A.S., 2024. Species traits and latitude mediate bird responses to forest edges globally. Landsc. Ecol. 39 (3), 1–14. https://doi.org/10.1007/s10980-024-01845-9.

Weerasena, L., Shier, D., Tonkyn, D., McFeaters, M., Collins, C., 2023. A sequential approach to reserve design with compactness and contiguity considerations. Ecol. Modell. 478 (January), 110281. https://doi.org/10.1016/j.ecolmodel.2023.110281.

Williams, B.A., Grantham, H.S., Watson, J.E.M., Alvarez, S.J., Simmonds, J.S., Rogéliz, C. A., Da Silva, M., Forero-Medina, G., Etter, A., Nogales, J., Walschburger, T., Hyman, G., Beyer, H.L., 2020. Minimising the loss of biodiversity and ecosystem services in an intact landscape under risk of rapid agricultural development. Environ. Res. Lett. 15 (1). https://doi.org/10.1088/1748-9326/ab5ff7.